

# IMPROVED CLASSIFICATION OF SPOT MULTI-SPECTRAL IMAGES FOR LAND-COVER TYPES EVALUATION ASSISTED BY DIGITAL ELEVATION MODEL (DEM) AND AERIAL PHOTOGRAPHS, A CASE STUDY

Saeid Noori Bushehri and Nooshin Khorsandian  
Department of GIS, Department of Photogrammetry,  
Assistant Director of GIS Dept., Remote Sensing Specialist  
National Cartographic Center (N.C.C.)  
Tehran, Iran

Commission VII, Working Group 2

**KEY WORDS: Remote Sensing, Land-Use, Classification, Image, SPOT, Multispectral, Spectral.**

## ABSTRACT:

The SPOT scene available for field work site, annually used by PHM3 & CAR3 students of ITC, was classified. The classified part is our area of interest for improved classification, whose existing classified map has been used as the ground truth. In conjunction with this, topographic data has been collected from mosaicked orthophotos which are subsequently digitized and overlaid to the composite SPOT image. The so formed topographic network superimposed to the landuse parcels visible on the satellite images is basically our tool for classification improvement as per case study title.

Assessment carried out to compare and contrast the conventional against improved classifications depicts that there is a great role played by introduction of both mosaicked orthophoto from scanned aerial photo imageries and DEM since the area in question is mountainous and of various landuse.

## 1. INTRODUCTION

The great advantage of having data available digitally is that it can be processed by computer either for machine assisted information extraction or for embellishment before an image product is formed. Remotely sensed image data of the earth's surface acquired from either aircraft or spacecraft platforms is readily available in digital format; specially the data is composed of discrete picture elements or pixels and radiometrically it is quantized into discrete brightness levels. Even data that is not recorded in digital form initially can be converted into discrete data by use of digitizing equipment such as scanners.

One of the applications of remotely sensed digital data, specially satellite imagery, is using them in *land cover classification*. There is two methods, namely *photo interpretation* and *quantitative analysis*. Photo interpretation is done by experienced operators to identify ground features and overall land cover.

Successful interpretation needs high quality images and expert operators. Since there is a need of supervision of human, it is too difficult and/or impractical to work in pixel level. We have to use computer to evaluate the satellite imagery with several bands in pixel level and with high radiometric resolution for accurate results of analysing. Computer assisted interpretation of remotely

sensed data is called *quantitative analysis*. In this method, at first land cover types or *spectral classes* are defined by the operators (users of the images), then by using of ground truth (data collected at the field operations) sample land cover types are identified in limited parts of images. In fact, we try to teach the computer the nature of different land cover types and their spectral specifications (training). In the next step, the trained computer starts to identify land cover types in the rest of images, namely a label is assigned to each pixel due to its spectral value. This kind of classification is called *classic* or *conventional classification*.

Present article is the result of a case study of authors at the end of a course, "Integrated Mapping and Geoinformation Production 3 (IGP3)," in 1993 at ITC, The Netherlands. The aim of the case study was to improve the conventional classification method by use of scanned aerial photos and existing DEM (Digital Elevation Model) of area.

Geometric distortions in satellite images can be related to number of factors, including

- (i) the rotation of the earth during image acquisition,
- (ii) the wide field of view of some sensors,
- (iii) the curvature of the earth,

- (iv) variation in platform altitude, attitude and velocity,
- (v) panoramic effects related to the imaging geometry, and
- (vi) relief displacement due to height difference.

There is possible to remove these distortions and the relief displacement due to height difference by introducing ground control points (GCPs) to images (georeferencing) and use of DEM respectively.

After all geometric corrections, orthoimages with a good accuracy come out as a result. They are also more accurate in classification than uncorrected images in conventional method. By use of aerial photos and the same DEM we are able to produce the orthophoto of the same area. This orthophoto can be the result of mosaicking of several photos covering the whole area, which are rectified separately. Topographic features (mainly landuse boundaries) are extracted from this mosaic. Ultimately, the landuse parcels visible on the satellite images are integrated in the topographic network. This network is basically our tools for the classification improvement.

A part of a full scene of the SPOT XS image with ground resolution of 20m was used in this case study. The area of interest was in south of France, and field data (ground truth) were collected by students of CAR3 of ITC in 1992.

### 1.1 Location

Our area of interest is located in southern France where annually fieldwork is conducted by Geoinformatics students, i.e. CAR3 and PHM3. It lies between 43 49'N and 43 54'N latitudes and 5 16'E and 5 20'E longitudes that covers the entire area of 10 x 10 km. This includes the Bonnieux municipality, with various land covers, partly mountainous and partly flat. Therefore height difference needs great care.

All steps in the case study were done by digital image processing techniques. The outputs could be either thematic maps or tables that are directly usable in a GIS.

### 1.2 Resources

This set of hardware and software were used in our study:

- IBM compatible personal computers
- Archimedes computer
- Colour laser printer
- Colour thermal printer
- Scanner
- ILWIS software
- ALEXANDER software
- Special purpose software

### 1.3 Data

These data sets were also used:

- Aerial photographs in 1:15000
- Part of SPOT XS full scene
- Topographic maps in 1:25000
- Field data
- DEM of area

## 2. PREPARATION AND PLANNING

At the beginning, we had to do the planning, namely identifying the data sets in the planning and defining the sources, way of supplying, formats of the data sets. For example, the area of interest in the region was identified by matching existing aerial photos, existing topographic maps, and field data. Then the SPOT XS scene that covered the whole area was ordered. We chose the SPOT XS image because its resolution was suitable for extracting parcel boundaries, roads, and other linear features.

The other step in planning was design of production line, defining of events in each step of production line, timing, identifying the tools and processes. The flow diagram of production line is depicted in figure 1.

### 2.1 List of events

- 2.0 Clipped orthophoto from column 178; center of photo (OR364) i.e. ORTHO36B
- 2.1 Mosaicked photo (MOS8 from ORTHO37B and OR364)
- 3.0 Area of interest (AREA)
- 3.1 Vector maps (ddbak1/2/3)
- 3.2 Edited vector map (FINAL)
- 9.0 GCP file (XSStie2)
- 9.1 Patched images (pat\_xs1/2/3)
- 9.2 Transformation coefficients and control points (outcoe.ctp and outcoe.coe)
- 9.3 Geo corrected images without relief displacement (s1/s2/s3); patched
- 9.4 Geo corrected images with relief displacement (s1st/s2st/s3st); patched
- 9.5 Unpatched 9.3
- 9.6 Unpatched 9.4
- 9.7 Stereo image
- 5.0 Train sample set
- 5.1 Classified map
- 5.2 Test sample set
- 5.3 Rasterized polygons map
- 5.4 Crossed output map
- 5.5 Aggregated classified map
- 5.6 Confusion matrix
- 4.0 Radiometric corrected images xss1rc, xss2rc and xss3rc

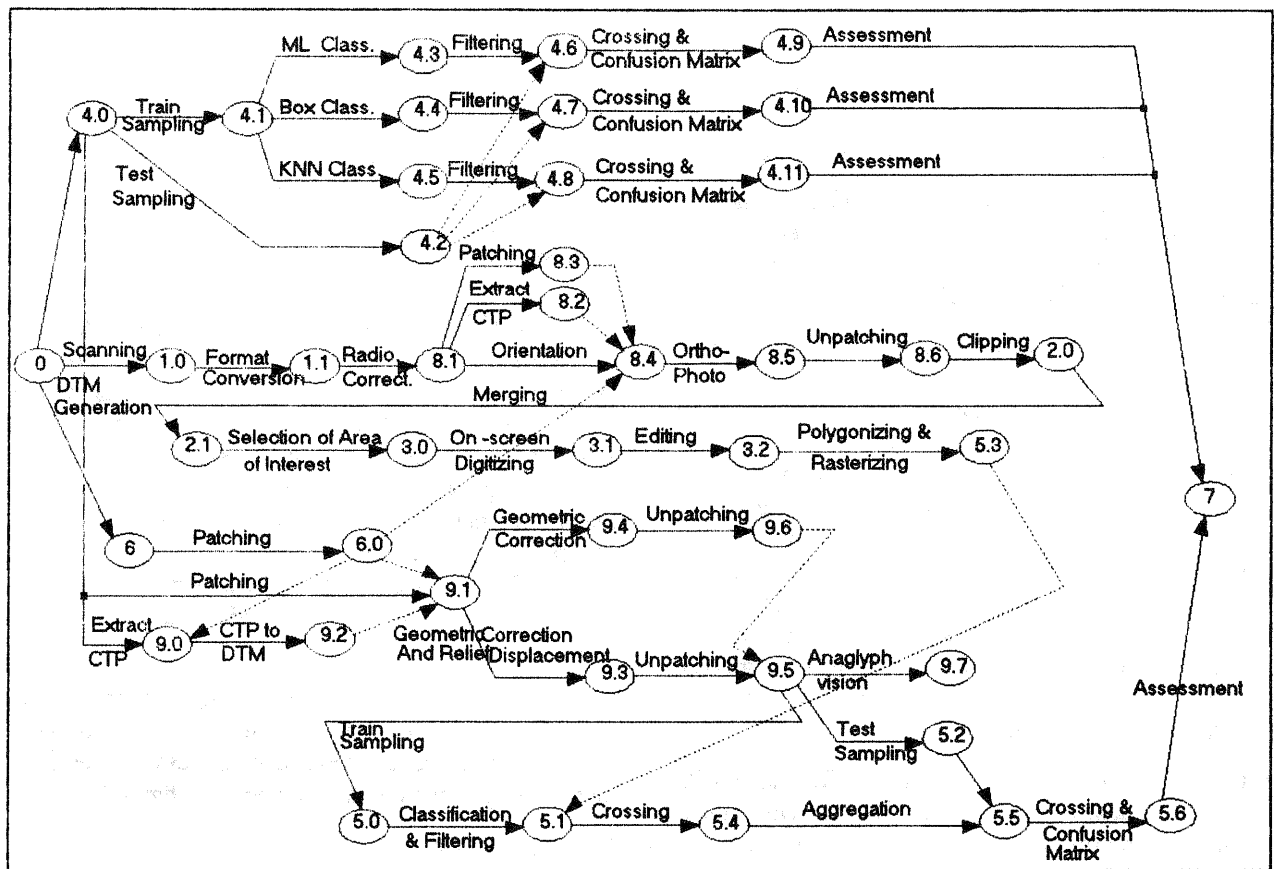


Figure 1 - flow diagram of production line

- 4.1 Train sample set (TRAIN2)
- 4.2 Test sample set (TEST2)
- 4.3 Classified image (ML17)
- 4.4 Classified image (BOX3)
- 4.5 Classified image (KNN5\_1)
- 4.6 Filtered classified image after ZERO majority and majority (ML17ZM)
- 4.7 Filtered classified image after ZERO majority and majority (BOX3ZM)
- 4.8 Filtered classified image after ZERO majority and majority (KNN5\_1ZM)
- 4.9 Crossing and confusion matrix (ML17ZM.MAT)
- 4.10 Crossing and confusion matrix (BOX3ZM.MAT)
- 4.11 Crossing and confusion matrix (KNN5\_1ZM.MAT)
- 1.0 Scanned photos (photo 36/37/38)
- 1.1 Converted scanned photos to ILWIS format (ph36/37/38)
- 8.1 Radiometric corrected photos (PH36RC, PH37RC, PH38RC)
- 8.2 Ground control points (GCP) file (T36N.DAT and T37NN.DAT)
- 8.3 Patched photos (PAT36 and PAT37)
- 8.4 Orientation files (OR36.ORI and OR37NN.ORI)
- 8.5 Patched orthophotos (ORTHO21 and ORTHO31)
- 8.6 Real orthophotos (ORTHO36B and ORTHO37B)
- 6 DTM
- 6.0 Patched DTM (PAT\_DTM)

### 3. IMPLEMENTATION OF PROCESSES AND EVENTS

#### 3.1 Conventional classification

This classification carried out to label the pixels in an image as representing particular ground cover types by suitable algorithms. In this case supervised classification has been adopted where nine classes have been categorised using three classifiers.

##### 3.1.1 Radiometric and geometric corrections

**3.1.1.1 Radiometric correction.** Linear stretch was done based on xss2 band with maximum stretch where xss1 and xss3 as slaves were stretched to conform with xss2 as master. Referring to the histogram data in table 1.

x s s 1			
0%	1%	99%	100%
33	37	86	173
x s s 2			
0%	1%	99%	100%
19	41	85	176
x s s 3			
0%	1%	99%	100%
28	49	86	131

table 1 - Histogram data of three bands

Thereafter, haze correction was done, i.e.

$$xss3rc = xss3 - 19; \quad (x3 = \$-19)$$

Eventually, we ended up with three radiometrically corrected images: xss1rc, xss2rc and xss3rc. These 3 bands were used to create the colour-composite image for conventional classification purpose but after geometric correction.

### 3.1.1.2 Geometric correction.

a) Panoramic distortion is negligible because the ratio of swath end element to nadir element is equal to 1.0013.

b) Earth rotation is considerable because the ratio of the shift across the swath to the swath width is equal to 0.050.

### 3.1.2 Train sampling

Eight classes were chosen to cover different land use to this area, as shown in table 2. Therefore, by choosing representative or prototype pixels from each of the desired sets of classes, these pixels are said to form training data. Training sets were established using the established (existing) ground truth map from a colour composite image on the ILWIS software. The training samples for a given class should lie in a common region enclosed by a boarder line or an edge. Unfortunately, our area of interest did not have clear defined boundaries to discriminate properly between different land covers due to composition of parcels of variable uses and outstanding height difference. Relief displacement has blurred the image to the extent that even edge enhancement does not help much to distinguish the parcels.

Class Name	Class Number
Forest	1
Orchard	2
Urban Area	3
Wasteland	4
Wasteland	5
Horticulture	6
Grass Field	7
Shrub	8

table 2 - Spectral classes of data

### 3.1.3 Error analysis

At the completion of conventional classification it is necessary to assess the accuracy of the results obtained. This was done by selecting a sample of pixels (test sampling) from remaining parcels and checking their labels against classes determined from training sampling, or crossing the two together to determine the accuracy. These results are expressed in a tabular form, often referred to as a confusion or error matrix.

Confusion matrix is shown in figure 2.

	1	2	3	4	5	6	7	8	uncl	ACC
1	32	0	0	0	0	0	0	1	0	0.97
2	82	0	0	0	0	0	0	0	0	0.00
3	0	0	68	1	7	2	0	0	0	0.67
4	51	0	0	0	0	0	0	30	0	0.00
5	0	0	9	3	1	0	25	0	0	0.03
6	0	1	0	4	0	0	0	0	0	0.00
7	0	0	0	0	8	0	0	0	0	0.00
8	16	0	0	0	0	0	0	1	0	0.06
REL	0.18	0	0.66	0	0.06	0	0	0.03		
average accuracy	= 24.08 %									
average reliability	= 14.42 %									
overall accuracy	= 29.82 %									

figure 2 - Confusion matrix of Maximum Likelihood classifier

## 3.2 Creation of DEM and its applications

In satellite images there is some amount of relief displacement and because of very high flying height and moving projection center, relief displacement across image lines is assumed to be very small and negligible but for pixels along the lines is not too small and it can be computed and removed.

In order to give corrections to all the pixels, the image observations are modified by introducing artificial errors (corresponding to relief displacement), errors that will be corrected while later resampling the whole image. This is the same as if the observations were made on a plane or flat ground. Therefore we need a DEM of area to remove relief displacement and obviously this DEM should be georeferenced, so we only need an affine transformation to remove relief displacement:

$$[X, Y]_{affine}^T \rightarrow [U, V]_{flat}^T \rightarrow [u, v]_{origin}^T$$

Having DEM, with help of some software we can first match our image to the DEM and then remove displacements of all pixels. The program CTPTODTM matches image to DEM and corrects the control points for relief and its usage is:

```
CTPTODTM xtie outcoe pat_dtm 5.6 -351 150
xtie: Name of our control points file
5.6: Looking angle.
-351: Beginning column.
150: Height reference.
```

The other program which name is GCD removes relief displacements. The DEM should be georeferenced and we match the images to the DEM with control points; It means that we have matched the image to the ground and after this step the program will read heights of points from DEM and it applies relief displacement for all pixels. We will also have a list of control points with their heights and their displacements. It should also be noted that relief displacement should be output driven.

Another application of DEM is to use it in creation of orthophoto and to do so we should patch the DEM with the program DTMPAT.

To create a DEM one can use SPOT PAN images (left

and right) and with image matching techniques and taking correlation between conjugate pixels, we can create a DEM. However, in this project since our aim was not creating DEM, but using it for different purposes, we used an existing DEM of the area that had already been created from digitizing contour lines in map and it was georeferenced and covered all our area of interest and thus we used this existing DEM.

### 3.3 Extraction of topographic data from scanned aerial photos

**3.3.1 Scanning photos and format conversion.** Aerial photos were scanned, to convert analog data into digital raster form. The required scanning resolution was chosen to suit both accuracy and storage capacity. Thus, the resolution of 100 dpi was appropriate. The raster data was in the TIFF format, therefore, in order to be used in the ILWIS system, it should get converted to MPD and MPI formats. The Data Conversion program was used for this process.

**3.3.2 Radiometric correction.** Sun angle correction is not applicable since we had only one channel information per scene. In this particular case, therefore only linear stretch was applied. For haze correction, we just shifted the brightness histogram of scanned photos to zero.

**3.3.3 Creation of orthophoto.** From the beginning, our area of interest was well defined in terms of both X- and Y- coordinates so only two scanned photos covered the whole area, therefore, the 2 orthophotos had to be created. For this matter, the planimetric coordinates were interpolated from existing map.

**3.3.3.1 Selection of Ground Control Points (GCP).** For a good georeferencing, GCPs need to be well distributed all over the image. For that matter, tie points are selected in the overlapping area. The 1:25000 map was used to acquire the coordinates of the well-defined points on both the map and photographs. The list of GCPs is shown in figure 3 for photo 36 and 37.

**3.3.3.2 Orientation of scanned photos.** ORIENT program performs an inner orientation based on the given relation of the fiducial marks provided the following data are given:

1. Control point file
2. Patched DEM file
3. Calibrated focal length

The transformation file will be delivered as output.

**3.3.3.3 Formation of orthophoto.** Once the orientation is satisfactory, the patched DEM, the patched scanned image, the output orientation files are required by ORTHOPHOTO program. The output image is still patch form. Thus it has to be unpatched which will deliver already to display digital orthophotos.

T36N.DAT						
pn	Col	Line	x	y	use	namees\$
1	845	461	0.115	0	1	east
2	430	876	0	-0.115	1	south
3	20	457	-0.115	0	1	west
4	436	42	0	0.115	1	north
-1						
pn	x	y	X	Y	use	
1	767.0	878.0	840338.0	3173500.0	1	
2	300.0	794.0	838525.0	3173638.0	1	
3	45.0	599.0	837450.0	3174500.0	1	
4	20.0	94.0	837250.0	3176575.0	1	
5	499.0	39.0	839300.0	3176863.0	1	
6	759.0	183.0	840375.0	3176250.0	1	
7	828.0	416.0	840650.0	3175288.0	1	
T37NN.DAT						
pn	Col	Line	x	y	use	namees\$
1	845	449	0.115	0	1	east
2	428	863	0	-0.115	1	south
3	19	443	-0.115	0	1	west
4	436	30	0	0.115	1	north
-1						
pn	x	y	X	Y	use	
1	667.0	771.0	838525.0	3173638.0	1	
2	395.0	575.0	837450.0	3174500.0	1	
3	217.0	792.0	836713.0	3173625.0	1	
4	189.0	497.0	836550.0	3174800.0	1	
5	360.0	74.0	837250.0	3176575.0	1	
6	725.0	185.0	838813.0	3176150.0	1	

figure 3 - GCP file

**3.3.4 Clipping and Merging.** After creation of orthophoto, both orthophoto 36 and orthophoto 37 were merged. The beginning of column of each orthophoto was removed to avoid some darkness after mosaicking. With the program MERGE, both orthophotos were merged together and meanwhile we defined an area of interest from the map and scanned photographs.

**3.3.5 On screen digitizing and Editing.** The displayed raster image on the screen, without using any hard copy, identified features were being digitized directly in the form of point and vector. With the advantage of zooming in and out, the cursor movements are adapted to the whole screen and the cursor becomes sensitive because of following the coordinates of the map placed on the digitizer. Several possibilities have been introduced with respect to the digitizer set up and the digitizing colors and even the existing codes are displayed when the user decides to change the mask and the codes of the segments. Thereafter, all the digitized data in the segment mode, are polygonized in order to make closed polygons. For this process, a unique number is assigned to each polygon according to the landuse separation.

## 4. IMPROVED CLASSIFICATION

### 4.1 Geometric correction

The following steps have been done:

- Patching the radiometrically corrected satellite images by use of PATCH program, since RAM does not have sufficient space to handle the whole image:

```
xss1rc □□□□□⇒ pat_xs1
xss2rc □□□□□⇒ pat_xs2
xss3rc □□□□□⇒ pat_xs3
```

- Producing a ground control points file (xtie.ctp) by use of ADDCOORD program in ILWIS. This file relates control points coordinates to satellite images. Our reference for ground coordinates was the existing map of area.

The control points file (xtie.ctp) is shown in figure 4.

Line%	Col%	X!	Y!	Delta_L&	Delta_C&
287	349	840050	3172900	-0.178833	-0.012420
194	385	841225	3174575	0.147858	-0.131226
139	222	838263	3176275	-0.138992	0.399384
158	162	837000	3176138	-0.008987	-0.418976
243	211	837538	3174300	0.178940	0.163208

figure 4 - Control points file

- Correction of control points for relief displacement. For doing that we used CTPTODTM program:

Usage:

```
CTPTODTM inctp outcoe dtm alpha col ref
Inctp: Control points from ILWIS (.ctp)
outcoe: Transformation coefficients for 'intodtm' (.coe)
dtm: ILWIS DEM file (.mpi and .mpd)
alpha: Looking angle in degrees
o: Vertical, pos: East
col: Image column to which alpha applies
ref: Reference height (no relief displacement)
```

The actual command which we entered was

```
CTPTODTM xtie outcoe pat_dtm 5.6 -351 150
```

The looking angle (5.6) and the column number (-351) have been extracted from the original image descriptions.

#### 4.1.1 Geometric correction with relief displacement.

We did the geometric correction for relief and transformation to the selected coordinate system (existing map of area) by use of GCD program:

Usage: GCD res in out coe dtm alpha col ref [pix]  
or

```
Usage: GCD res in out coe pix
res: resampling method
n: nearest neighbour
b: bilinear
in: patched input image (.mpi and .mpd)
out: patched output image (.mpi and .mpd)
coe: coefficient file (.coe)
dtm: patched ILWIS DEM file (.mpi and .mpd)
alpha: looking angle
o: vertical
pos: east
col: image column to which alpha applies
ref: reference height (no relief displacement)
pix: output pixel size (m)
```

The actual commands that we entered were:

```
GCD n pat_xs1 pat_s1 outcoe pat_dtm 5.6 -351 150 20
GCD n pat_xs2 pat_s2 outcoe pat_dtm 5.6 -351 150 20
GCD n pat_xs3 pat_s3 outcoe pat_dtm 5.6 -351 150 20
```

**4.1.2 Geometric correction without relief displacement.** We executed GCD program with the original images and the original control points to produce the anaglyph vision:

```
GCD n pat_xs1 pat_s1st xtie 20
GCD n pat_xs2 pat_s2st xtie 20
GCD n pat_xs3 pat_s3st xtie 20
```

Then we unpatching all images to ILWIS format by use of UNPATCH program:

```
UNPATCH pat_s1 s1
UNPATCH pat_s2 s2
UNPATCH pat_s3 s3
UNPATCH pat_s1st s1st
UNPATCH pat_s2st s2st
UNPATCH pat_s3st s3st
```

**4.1.3 Anaglyph stereo vision.** We produced a color-composite image by use of COLORCMP program in ILWIS:

```
COLORCMP s1st s1 s1 $; or
COLORCMP s2st s2 s2 $; or
COLORCMP s3st s3 s3 $;
```

After completion of one of these commands, and with help of a pair of anaglyph glasses, we are able to see the stereo model of area on the screen.

## 4.2 Classification

**4.2.1 Train and test sampling.** We divided the ground truth into two separate sets, one for training and one for testing the classifiers.

**4.2.2 Crossing and error analysis.** Using the program "crossing", cross tables were generated between the test samples, e.g., TEST3, and their corresponding geometrical corrected conventional classified satellite image. Confusion matrices are shown in figure 5.

	1	2	3	4	5	6	7	8	uncl	ACC
1	235	0	0	0	0	0	0	1	97	0.71
2	0	193	0	0	0	0	0	0	0	1.00
3	0	0	0	0	24	0	0	106	192	0.00
4	0	0	0	0	1	62	0	0	119	0.00
5	0	120	0	0	141	32	22	5	209	0.33
6	0	73	0	0	41	0	0	0	6	0.00
7	28	3	0	0	0	0	2	0	21	0.04
8	0	0	0	2	48	0	0	0	70	0.00
REL	0.69	0.69	?	0	0	0.55	0	0.08		
average accuracy	= 26.00 %									
average reliability	= 31.67 %									
overall accuracy	= 32.31 %									

figure 5 -Confusion matrix of Maximum Likelihood classifier with zero majority filtering

### 4.3 Polygonizing and Rasterizing

**4.3.1 Vector to polygon conversion.** All the digitized data were in segment mode. The polygonization process was done to make closed polygons. In ILWIS system we used the program called "polygonizing" to perform this task. For this process, a unique number was assigned to each polygon.

SEGMENTS		
FINAL.SEG	<i>polygonizing</i>	FINAL.DAT
FINAL.SLG	ooooooooo↪	FINAL.POL
FINAL.CRD		FINAL.TOP
		FINAL.PLG

**4.3.2 Polygon to raster conversion.** These polygonized parcel boundaries are still in vector mode. In order to process these data along with the satellite data, they were converted to a raster form. In ILWIS system we used the program called "rasterization" to perform this task. The program assigned an arbitrary color to each polygon as a label.

FINAL.DAT		
FINAL.POL	<i>rasterization</i>	FINAL.MPD
FINAL.TOP	ooooooooo↪	FINAL.MPI
FINAL.PLG		FINAL.INF

By selection of the raster map in the "read pixel from screen" menu information of all polygons can be retrieved simultaneously. Moreover we should change the name of the attribute information stored in ILWIS table file (e.g., FINAL.INF change to FINALSAV.INF).

### 4.4 The Final step

**4.4.1 Crossing rasterized polygons and result of classification.** These rasterized polygons (FINAL.\*) were crossed with the geometrically corrected conventional classified satellite image (e.g., ML3-23Z). Crossing can be done with the program "crossing" in the ILWIS system.

**4.4.2 Aggregation.** The program performs different types of aggregation functions on the pixel values listed in the cross table. Aggregation functions were applied to the pixel values of the second map (e.g., ML3-23Z) per pixel value of the first map (e.g., FINAL). At this level, the most occurring (predominant) pixel value within each polygon is assigned to that polygon. This process was carried out by using of the program "mapcalc" as follow:

MCALC IMP := CROSS.PREDCOL[FINAL];

**4.4.3 Crossing and error analysis.** This IMP is generated under MCALC and crossed by the test sample classes ,e.g., TEST3. Confusion matrix is shown in figure 6.

	1	2	3	4	5	6	7	8	unct	ACC
1	21	4	0	0	2	0	1	16	0	0.45
2	0	3	0	22	0	0	0	0	0	0.08
3	2	12	0	0	0	0	0	0	0	0.89
4	0	12	0	0	0	0	0	0	0	0.00
5	0	0	0	0	31	0	0	0	0	1.00
6	0	0	0	0	9	0	0	0	0	0.00
7	0	0	0	0	4	0	0	0	0	0.00
8	5	0	0	0	0	0	0	14	0	0.74
REL	0.89	0.69	?	0	0	0.55	0	0.08		
average accuracy	= 40.57 %									
average reliability	= 34.41 %									
overall accuracy	= 54.67 %									

figure 6 -Confusion matrix of Maximum Likelihood classifier after aggregation

As it can be seen, by developing the improved classification method we could reach to overall accuracy of 54.67% in compare with 29% in conventional method.

## 5. CONCLUSION

Scanned aerial photos have the advantage of showing edges to separate different earth cover of variable landuse. For that matter, the classification is improved because one can very easily recognize all features including point and line, where the 100 dpi was used as the resolution of photo images.

For non-flat terrain, it is essential to consider the DEM because the question of relief displacement should not be overlooked since it adversely affects the geometry of satellite images. If both factors are put into consideration in the correct way, the classification is trivially improved to a very good extent. The scanned aerial photos and DEM have facilitated the classification of satellite imageries though it has been difficult to be depicted in terms of technical documents.

The problem in matching of vector data and raster data has led us to realising that DEM had propagated errors because topo data almost matched with SPOT raster data on flat terrain but the some discrepancies were visually noticed on mountainous terrain to disclose relief displacement that increases with height.

In aggregation process in each parcel, we assigned the label of dominant pixels to all pixels within that parcel. If we consider everything perfect, then we can expect the classification being improved.

## 6. RECOMMENDATION

Hereby, we consider the factors that increase the accuracy of land-cover type elevation. Accuracy and attention in collecting up-to-date ground truth data have the great importance in classification. Out-dated or inaccurate ground truth data, besides the changes of land-cover in different seasons, are the main problems. The best thing is to use ground truth data, aerial photographs, and satellite images of the same time (or at least at the same period of successive years). Of course, there are some serious problem to obtain this set of data.

First of all, providing the annual ground truth data is time-consuming and involves some expense. However, it might be managed in relevant student fieldwork with guide of experienced people, as ITC does.

The second problem is to obtain up-to-date aerial photographs of area. Having the regular aerial photos is too expensive. There is possibility to use old photographs in areas with no great change in parcel shapes.

The third problem is access to satellite imagery. Normally, there are some official organizations or companies in charge of presenting satellite images. However, there must be the possibility to order the images in growing seasons of vegetation.

Having an accurate DEM is the most important thing among the others. The more the accurate DEM, the more accurate the geometric correction process we can do. In this case study, we used the DEM that had been compiled from digitizing and interpolation of 1:25000 map contours. It seems that this DEM does not have adequate accuracy for performing the necessary corrections. This lack of accuracy in DEM causes unmatched respective polygons and parcels in the overlaid images. Unmatched polygons and parcel, then cause uncertainty in classification of images.

## References

Richards, John A., 1993. Remote Sensing Digital Image Analysis, Springer-Verlag, Berlin.

Russ, John C., 1992. The Image Processing Handbook, CRC, Florida.

Ellis, E.C. Statistical Pattern Recognition - Classification and Feature Selection in Image Processing, ITC Lecture note, The Netherlands.

Huurneman, G.C. Geometric Corrections of Digital Images, ITC Lecture note, The Netherlands.

Kostwinder, H.R. and Bakx, J.P.G., 1991. Radiometric Corrections of Digital Images, ITC Lecture note, The Netherlands.

Gorte, B.G.H. Local Operators/Filters and Structural Pattern Recognition, ITC Lecture note, The Netherlands.

Bakx, J.P.G., 1991. Colour Coding and spectral Feature Extraction, ITC Lecture note, The Netherlands.

Horn, J., 1992. Primary Data Acquisition, ITC Lecture note, The Netherlands.